

Multi-Parameter Optical Image Interpretations Based on Self-Organizing Mapping

Christian. D. Klose^a, A.K. Klose^b, U. Netz^c, A. Scheel^d, J. Beuthan^c, Andreas H. Hielscher^{a,b}

^aDepartments of Biomedical Engineering and ^bRadiology, Columbia University,
351 Engineering Terrace, New York, NY 10027

^cInstitut für Medizinische Physik und Lasermedizin, Charité - Universitätsmedizin Berlin,
Fabeckstraße 60-62, 14195 Berlin, Germany

^dDept of Nephrology and Rheumatology, George-August-University Göttingen, Germany

ABSTRACT

We found that using more than one parameter derived from optical tomographic images can lead to better image classification results compared to cases when only one parameter is used. In particular we present a multi-parameter classification approach, called self-organizing mapping (SOM), for detecting synovitis in arthritic finger joints based on sagittal laser optical tomography (SLOT). This imaging modality can be used to determine various physical parameters such as minimal absorption and scattering coefficients in an image of the proximal interphalangeal joint. Results were compared to different gold standards: magnet resonance imaging, ultra-sonography and clinical evaluation. When compared to classifications based on single-parameters, e.g., absorption minimum only, the study reveals that multi-parameter classifications lead to higher classification sensitivities and specificities and statistical significances with p-values <5 per cent. Finally, the data suggest that image analyses are more reliable and avoid ambiguous interpretations when using more than one parameter.

Keywords: Optical Tomographic Imaging, Classification, Artificial Intelligence, Self-Organizing Maps

1. INTRODUCTION

Sagittal laser optical tomography data (SLOT) has recently been employed to detect rheumatoid arthritis (RA) in finger joints.¹ This method relies on series of transillumination measurements that are used as input to a model based image reconstruction code.^{2,3,4,5} The code produces cross sectional images of the absorption and scattering properties in the proximal interphalangeal (PIP) joints of the hands. Using data from 78 PIP joints, including data from patients diagnosed with RA as well as healthy volunteers, Scheel et al. investigated how various single parameters such as minimum or maximum values of the absorption coefficient μ_a and scattering coefficient μ_s in an area of interest within a given image can be used to distinguish between affected and non-affected joints. Statistical analysis of the data revealed that, when using the minimum absorption coefficient $\min(\mu_a)$, sensitivity and specificity values of approximately 0.70 can be reached, while other parameters such as $\max(\mu_a)$ or $\min(\mu_s)$ yielded poorer classification results. In this study we explore if combining two or more parameters increases sensitivity and specificity. To test our hypothesis we used an extended data set of 178 images of PIP joints including the aforementioned data set. All data were gathered in accordance with IRB guidelines, and patients and healthy volunteers provided informed consent prior to examination.

2. DATA

Optical measurements on the finger joints were performed with a SLOT imaging system, described in detail in previous studies.^{3,6} The system is comprised of a single laser diode and single a silicon photo detector, which are scanned independently along a sagittal plane across the PIP joint. The transillumination data of multiple scans are input to a model-based iterative image reconstruction algorithms, which uses the equation of radiative transfer (ERT) to model light propagation in tissue. The resulting SLOT images show the spatial distribution of two different optical properties, μ_a and μ_s (Fig 1.). A region of interest (ROI) was defined within the SLOT images to extract different parameters for

further analysis. Minimum-value $\min(\cdot)$, maximum-value $\max(\cdot)$, maximum-to-minimum-ratio and the statistical variance $\text{var}(\cdot)$ of μ_a and μ_s values were drawn from the ROI in each of the 178 images. In addition to the optical tomographic images, the fingers were also evaluated by magnet resonance imaging (MRI) and ultrasound imaging (US). Furthermore, a detailed examination by a physician led to an independent clinical diagnosis (CL).

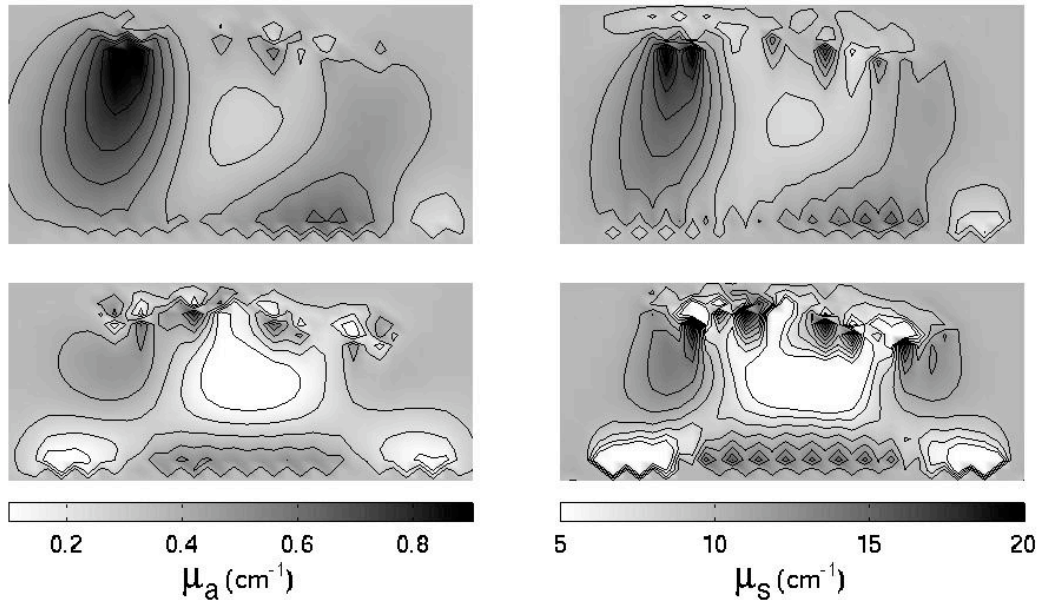


Fig. 1: Examples of absorption and scattering images in a sagittal plane through a PIP finger joint affected by RA (top row) and a finger not affected by RA (bottom row). The images in the top row display a 35mm by 20mm region, while the bottom rows shows images of 35mm by 17mm.

3. METHODOLOGY

3.1 3.1 General Concept

To analyze the data we implemented an artificial intelligent methodology commonly referred to as Self-Organizing Mapping (SOM). This approach allows classifying more than one parameter simultaneously. Instead of determining the mean and standard deviation of just one parameter (e.g., $\min(\mu_a)$) for healthy and affected patient groups, and determining the significance of the difference between the two groups, the SOM approach allows to combine $\min(\mu_a)$, $\max(\mu_a)$, $\min(\mu_s)$, $\max(\mu_s)$, etc. Using SOM can transform feature vectors of arbitrary dimension into simplified generally 2-dimensional discrete maps (Kohonen layer).^{7,8} This type of neural network utilizes an unsupervised learning method, known as competitive learning in the field of neural information processing. It is useful for analyzing, in particular, interpreting complex data with a-priori unknown relationships or interdependencies,⁹ such as in case of the SLOT data.

The finger joint data were analyzed (clustered) by SOM-networks of different Kohonen layer sizes. The outcomes were compared with benchmarks (gold standards) resulting from expert interpretations of magnet resonance images (MRI), ultrasound images (US), and clinical diagnosis (CL). This comparison can ensure to what extent features (e.g., min, max) of the measured data (μ_a and μ_s) can be described by class labels (“affected” and “non-affected”) of the given gold standards. Results of the discrimination can be visualized in the 2-dimensional Kohonen layer with neurons (groups) showing class labels based on a selection criterion as shown in Fig. 2C.

The frequency per class describes the number of identified finger joints. Different multi-dimensional parameter spaces of μ_a and μ_s , which are separated by the SOM in to sub-groups (clusters), consist varying number of “affected” and “non-

affected” finger joints, although the physical optical data (μ_a and μ_s) are similar. The above mentioned criterion determines units (clusters) within the μ_a - μ_s -spaces that represent a certain class very well or less good.

3.2 Meta-Algorithm

One objective was to develop a meta-algorithm that is able to classify and interpret the SOM classifications of the given feature vectors with respect to dimensionality of the feature space $n \leq 4$, the SOM-architectures ($m \times m$), the independent gold standards (e.g., MRI, US, CL) and wit respect to the interpretation accuracy (class labels) $\{c_0 = \text{“not affected”}, c_1 = \text{“affected”}\}$ for each standard.

The algorithm is summarized as follows:

```

Set dimensionality n feature space  $X_n$ 
Set classification accuracy of the SOM  $M = 10$ 
Set interpretation accuracy c
Set interpretation standards  $S(c)$ 
Generate an ensemble of L  $m \times m$  SOM-networks
BEGIN Loop for each SOM( $m \times m$ )  $l = 1 \rightarrow L$ 
    Separate all  $x_n$  into  $m \times m$  sub-groups  $w_n$ 
    Calculate sensitivity  $S_e$  and  $S_p$ 
    Calculate Youden index  $Y(S_e, S_p)$ 
END Loop
Determine  $\arg \max(Y)$  as best interpreted classification result
  
```

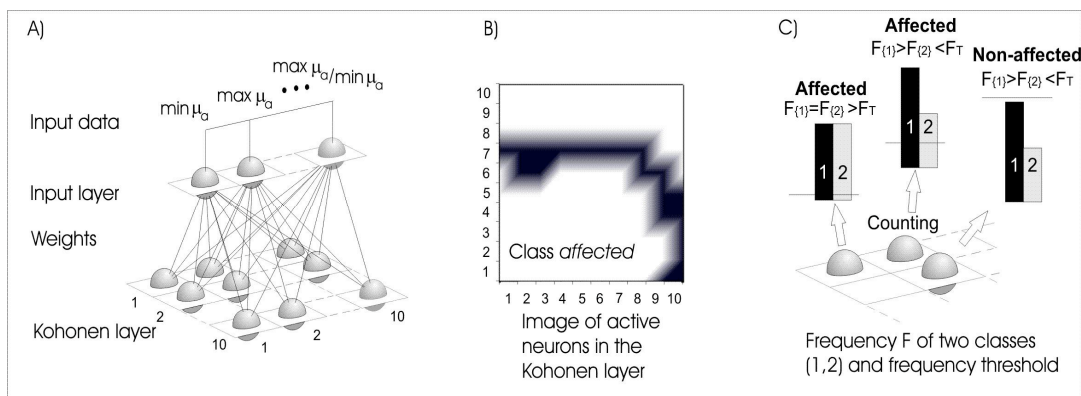


Fig. 2. Scheme for multi-parameter classifications based on SOM: A) Structure of a SOM neural network, B) Image of active neurons representing the class “affected” within the Kohonen layer after discrimination of the given input data, C) Frequency determination and final interpretation of the classes affected (black) and non-affected (gray) based on a variable frequency threshold F_T .

4. RESULTS AND DISCUSSION

The classification problem for detecting rheumatic arthritis in finger joints was conducted based on μ_a and μ_s values of the SLOT data by combining up to four different parameter, e.g., $\min(\mu_a)$, the ratio $\max(\mu_a)/\min(\mu_a)$ and $\text{var}(\mu_a)$. Multi-dimensional input data were classified based on an $m \times m$ SOM neural information processing approach. Moreover, the application of sensitivity-specificity-curves (ROC-curves) was used as a way to model interpretation (classification) results with respect to the observer’s subjectivity (frequency threshold value). ROC-curves describe the sensitivity and the specificity of a classification result as functions of an expert’s gold standard and frequency thresholds varying between 0 and 1.¹⁰ As above mentioned, a finger was classified as affected (or non-affected) when the frequency of this

class for a certain neuron in the Kohonen layer of the SOM network was larger than the chosen threshold value and larger than the exclusive class non-affected (or affected). Thus, the neuron represents a group of data point with similar combined physical features.

Different parameter combinations result in varying sensitivities and specificities for each gold standard as result of changing frequency thresholds as well as dimension of the μ_a - μ_s -parameter spaces and size of the Kohonen layers (Fig. 3). Some classifications can lead to higher sensitivities, whereas others to higher specificities. For each benchmark, we calculated the sensitivity (SE) and specificity (SP) for the point on the ROC-curve with the highest Youden index Y , which characterized the point on the curve closest to sensitivity=specificity=1.¹¹ Thus, the interpretation quality is 1- Y (Fig. 3).

The best results were based on the 3-D feature space $\{\min(\mu_a), \max(\mu_a)/\min(\mu_a), \text{var}(\mu_a)\}$. If MRI is used as benchmark, which is widely accepted in the clinical field as gold standard for RA diagnostic, we find $S_e=1.00$, $S_p=0.87$, and $Y=0.13$ with a statistical significance of $p<5$ per cent. These are excellent values that put SLOT technology clearly in the range of clinically useful diagnostic methods. The same S_e , S_p , and Y values are found when CL is used as benchmark, while using US as gold standard yields, $S_e=1.00$, $S_p=0.88$, and $Y=0.12$.

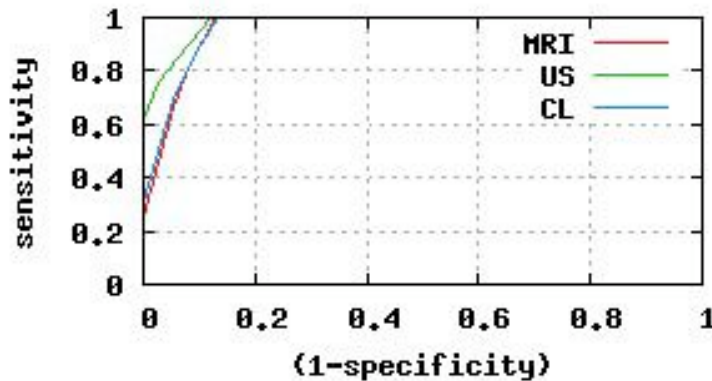


Fig. 3: ROC-curves describe the quality of an interpretation of $\{\min(\mu_a), \max(\mu_a)/\min(\mu_a), \text{var}(\mu_a)\}$ for three different benchmarks (gold standards), magnetic resonance imaging (MRI), ultrasound imaging (US), and clinical diagnostic (CL). Best results are based on a 7×7 SOM and data set.

Results also show that the classification quality is uncorrelated to the dimensionality of the parameter space. Thus, many combined parameters do not necessarily determine a high separability of affected and non-affected fingers. Ideally, parameters should be chosen based on their physical relevance. For example, we found that non-affected fingers show high statistical variances in the μ_a -space. Such information, which was a-priori not available, could be determined based on the SOM approach.

Specificity and sensitivity are also uncorrelated to the size of the Kohonen layer that determines the precision of a classification (Fig. 4). In detail, Kohonen layer of $3 \times 3=9$ neurons can represent approximately 1/10 of 100 data points in a given data set. Each of the resulting 9 clusters contains similar data points (from a physical view point), whereas their class labels might be dissimilar (low specificity or sensitivity) or similar (high specificity or sensitivity) according to a given gold standard and frequency threshold. A $5 \times 5=25$ Kohonen layer separates the 100 data points with a 250% higher precision than the 3×3 SOM. Hence, each neuron represents a smaller set of physical similar data points. Thus, the number of class members and the class frequency of this cluster (neuron) changes as well as sensitivity and specificity values. For example, a neuron of the 3×3 SOM represents a cluster of 15 data points with 8 affected fingers (53%) and 7 non-affected fingers (47%). On the other hand, the same neuron of the 5×5 SOM represents a cluster that is now consisting of 10 data points with 3 affected fingers (30%) and 7 non-affected fingers (70%). The other 5 data points may now belong to other clusters, since the classification precision increased. Finally, these class frequency changes can alter the resulting ROC-curves significantly and non-linearly.

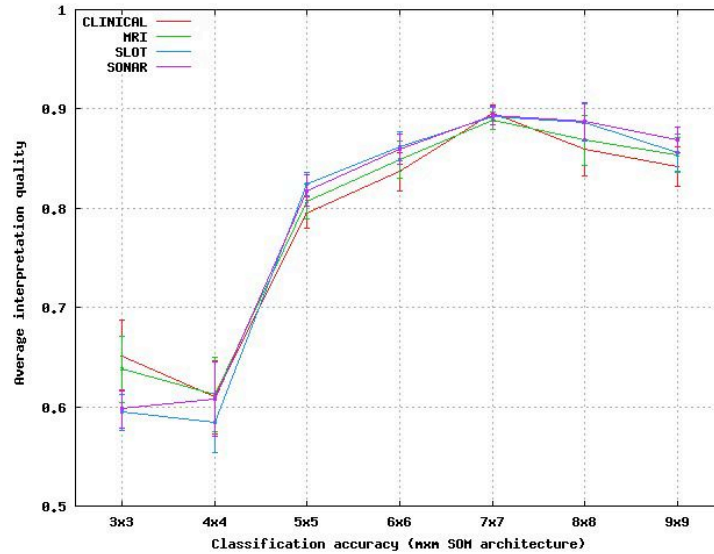


Fig. 4: Interpretation quality (1-Youden index) as a function of the interpretation accuracy (size of the SOM-network) and the gold standards.

5. CONCLUSION

The identification of rheumatoid arthritis in finger joints is possible by analyzing sagittal laser optical tomography images when compared to other imaging techniques. Up to four parameters in combination of the absorption coefficient μ_a and scattering coefficient μ_s were considered as part of this study. Multi-dimensional parameter spaces were analyzed by an artificial intelligent classification approach, called Self-Organizing Mapping (SOM). Results of this study suggest that sensitivities and specificities of the multi-parameter image classifications are uncorrelated to the dimensionality of the parameter spaces. Thus, combinations of more than 3 parameters between the μ_a and μ_s , for instance, could lead to very smaller sensitivities and specificities. However, proper parameter combination $\{\min(\mu_a), \max(\mu_a)/\min(\mu_a), \text{var}(\mu_a)\}$ can be determined that result into higher sensitivities and specificities when compared to single-parameter classifications and different expert interpretations based on magnet resonance images (MRI), ultrasound images (US), and clinical diagnosis (CL). Using MRI as clinical gold standard we find that sensitivity and specificity values up to 0.87 and 1 respectively can be achieved. This makes SLOT imaging a competitive diagnostic tool for the detection of RA in finger joints.

6. ACKNOWLEDGMENTS

This work was supported in part by a grant (#2R01 AR46255) from the National Institute of Arthritis and Musculoskeletal and Skin Diseases (NIAMS), which is part of the National Institutes of Health.

REFERENCES

¹ Scheel A.K. M. Backhaus A. D. Klose B. Moa-Anderson U. J. Netz K-G.A. Hermann J. Beuthan G.A. Müller G.R. Burmester A.H. Hielscher "First clinical evaluation of sagittal laser optical tomography for detection of synovitis in arthritic finger joints," *Ann. Rheum. Dis.* **64**, 239-245 (2005).

² Klose, A. Beuthan J. Mueller G., Investigations of RA-diagnostics applying optical tomography in frequency domain, in: *Optical and Imaging Techniques for Biomonitoring*, H.J. Foth, R. Marchesini, and H. Podbielska, eds., SPIE Proc. **3196**, 194-204 (1997)

- ³ Klose A.D. A.H. Hielscher K.M. Hanson J. Beuthan "Two and three-dimensional optical tomography of a finger joint model for diagnostic of rheumatoid arthritis," Proc. SPIE Int. Soc. Opt. Eng. **3566**, 151–60 (1998)
- ⁴ Klose A.D. Netz U. Beuthan J. Hielscher A.H., Optical tomography using the time-independent equation of radiative transfer. Part I: Forward model, J. Quant. Spectrosc. Radiat. Transfer **72(5)**, 691-713 (2002)
- ⁵ Klose A.D. Hielscher A.H., Optical tomography using the time-independent equation of radiative transfer. Part II: Inverse model, J. Quant. Spectrosc. Radiat. Transfer **72(5)**, 715-732 (2002)
- ⁶ Hielscher A.H. A.D. Klose A. Scheel B. Moa-Anderson M. Backhaus U. Netz J. Beuthan "Sagittal Laser Optical Tomography for Imaging of Rheumatoid Finger Joints," Physics in Medicine and Biology **49(7)**, 1147 - 1163 (2004).
- ⁷ Kohonen T. "Self-organizing formation of topologically correct feature maps," Biol. Cyb. **43(1)**, 59-69 (1982).
- ⁸ Kohonen T. "Self-Organizing Maps" 3rd edition, Springer, Berlin (2001).
- ⁹ Klose C.D. "Self-Organising Maps for Geoscientific Data Analysis: Geological Interpretation of Multi-dimensional Geophysical Data," Computational Geosciences, **10(3)**, 265-277 (2006).
- ¹⁰ Metz C.E. and X.C. Pan "Proper binormal ROC curves: Theory and maximum likelihood estimation," Journal of Mathematical Psychology **43**, 1–33 (1999).
- ¹¹ Youden WJ. "Index rating for diagnostic tests," Cancer **3**, 32–5 (1950).